

# Host-isotope effect on the localized vibrational modes of oxygen dimer in isotopically enriched silicon

Daisuke Tsurumi<sup>a</sup>, Kohei M. Itoh<sup>a,\*</sup>, Hiroshi Yamada-Kaneta<sup>b</sup>

<sup>a</sup>Department of Applied Physics and CREST-JST, Keio University, 3-14-1 Hiyoshi Kohoku-ku, Yokohama-shi Kanagawa-ken 223-8522, Japan

<sup>b</sup>Fujitsu Ltd., Atsugi Laboratories, 10-1, Morinosato-Wakamiya, Atsugi 243-0198, Japan

## Abstract

Local vibrational modes of oxygen dimers in silicon have been investigated using naturally available silicon (<sup>nat</sup>Si) and isotopically enriched <sup>29</sup>Si and <sup>30</sup>Si crystals. Infrared absorption spectroscopy of <sup>nat</sup>Si revealed two pairs of peaks originated from the oxygen dimers, a pair A at 1012 and 1060 cm<sup>-1</sup> and a pair B at 1105 and 1136 cm<sup>-1</sup>, whose frequencies shifted when the mass of the silicon host atoms was changed. The observed frequency shifts of both A and B can be accounted for with a simple linear chain calculation assuming two previously proposed atomic configurations known as staggered and skewed dimers. Further analysis, based on the degree of contribution from the second and beyond nearest neighbor silicon masses, allows us to assign the pair B as the skewed dimer absorption peaks while the pair A as the staggered dimer absorption peaks.

© 2005 Elsevier B.V. All rights reserved.

PACS: 61.72.-y; 63.20.Pw; 78.30.Am

Keywords: Isotopically enriched silicon; Oxygen dimer; LVM; Linear chain calculation

## 1. Introduction

Localized vibrations of impurity complexes in semiconductors occur when the mass of atoms forming the complexes is much smaller than that of the host atoms. Oxygen is an important choice for investigations of localized vibrational modes (LVM) in silicon because (1) it is the most common impurity in the silicon technology and (2) it forms a large number of complexes with lattice defects and other impurity atoms in the course of thermal cycles associated with silicon integrated circuit processing. Introduction of oxygen is almost unavoidable in processing of state-of-the-art integrated circuits based on silicon. Hence, an in-depth understanding of the properties of oxygen, including its LVM, may lead to development of new characterization tools for oxygen in silicon [1–4].

Oxygen in silicon single crystals can exist as isolated oxygen atoms, oxygen molecules, and oxygen complexes. For the case of the complexes, oxygen atoms form bonds

with host atoms, shallow impurities, transition metals, hydrogen, carbon, etc [2–4]. The local structures of such defects have been determined using a variety of characterization tools such as DLTS, EPR, and FTIR. When FTIR is employed, the involvement of oxygen is very often confirmed by observation of the frequency shift of the LVM upon substitution of <sup>16</sup>O by <sup>18</sup>O. The ratio between the mode frequencies for <sup>16</sup>O and <sup>18</sup>O is close to  $3\sqrt{2}/4$ . In many oxygen-related complexes, the oxygen atoms form covalent bonds with host atoms. In such cases, the neighboring host atoms will participate weakly in the local mode oscillation and therefore, a small frequency shift will result if the isotope of the host atom is changed. However, the isotopic composition of naturally available silicon (<sup>nat</sup>Si) is always fixed at 92.2% <sup>28</sup>Si, 4.7% <sup>29</sup>Si, and 3.1% <sup>30</sup>Si. In order to overcome this limitation, we have grown nearly monoisotopic crystals of the three stable isotopes <sup>28</sup>Si, <sup>29</sup>Si, and <sup>30</sup>Si, and thereby added a new degree of freedom to LVM studies in silicon [5,6]. We took advantage of this in the past and investigated the effect of host silicon isotopes on LVMs of oxygen [7,8], carbon [8], and hydrogen [9].

\*Corresponding author. Tel.: +81 45 566 1594; fax: +81 45 566 1587.  
E-mail address: [kito@appi.keio.ac.jp](mailto:kito@appi.keio.ac.jp) (K.M. Itoh).

The present study focuses on the host-isotope effect of silicon on the oxygen dimer LVMs since the oxygen dimer is one of the most extensively studied oxygen complexes as the first step for oxygen aggregations in the silicon thermal process [10–16]. Experimentally, three LVM frequencies of oxygen dimers, 1012, 1060, and 1105  $\text{cm}^{-1}$ , have been found in  $^{\text{nat}}\text{Si}$  by FTIR [14]. Based on these experimental values, Pesola et al. [15–17] suggested structures of oxygen dimers using first-principle calculation. According to them, two structures, so-called staggered and skewed oxygen dimers (Fig. 1), having asymmetric bond lengths and angles are stable. The absorption pair A (1012 and 1060  $\text{cm}^{-1}$ ) and absorption pair B (1105 and 1136  $\text{cm}^{-1}$ ) are assigned as staggered and skewed oxygen dimers, respectively. Furthermore, experimental measurements of the frequency shifts of the LVMs of oxygen dimers in  $^{18}\text{O}$ -doped Si gave additional support for the assignments of oxygen dimers [13,15]. Therefore, it is of great interest to extend the study to the host-isotope effect to evaluate the consistency of the assignments.

## 2. Experiments

We have investigated LVMs of oxygen dimers in isotopically enriched  $^{29}\text{Si}$ ,  $^{30}\text{Si}$ , and  $^{\text{nat}}\text{Si}$ .  $^{\text{nat}}\text{Si}$  contains  $^{28}\text{Si}$  (92.2%),  $^{29}\text{Si}$  (4.7%), and  $^{30}\text{Si}$  (3.1%). The isotopically enriched  $^{29}\text{Si}$  and  $^{30}\text{Si}$  had the enrichment of  $^{29}\text{Si}$  (97.1%) and  $^{30}\text{Si}$  (98.7%). The isotopic composition, oxygen concentration, and carbon concentration for each sample are summarized in Table 1. The isotopic composition of silicon isotopes were determined by secondary-ion mass spectrometry (SIMS). The concentrations of oxygen and carbon were determined by the intensity of well-known IR absorption bands [18]. The measurements were carried out using a BOMEM DA-8 Fourier transform spectrometer equipped with a Globar light source, a KBr beam splitter, and a HgCdTe detector. The thickness of each sample is about 10 mm. The sample was kept in an Oxford Optistat Cryostat (continuous He flow) with ZnSe windows. The experiments were performed at room temperature (about 293 K) and 5 K. The resolution was 1.0 or 0.5  $\text{cm}^{-1}$ , and

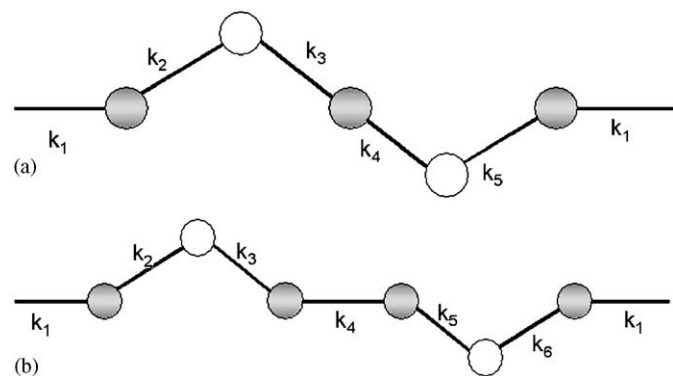


Fig. 1. Proposed structures of the (a) staggered oxygen dimer and (b) skewed oxygen dimer in silicon. Gray and white balls are silicon and oxygen atoms, respectively.  $k_1$ – $k_6$  denote the force constants.

Table 1

Isotopic composition and the oxygen and carbon concentrations of the samples employed in the present study

Sample	$^{28}\text{Si}$ (%)	$^{29}\text{Si}$ (%)	$^{30}\text{Si}$ (%)	Oxygen ( $\text{cm}^{-3}$ )	Carbon ( $\text{cm}^{-3}$ )
$^{29}\text{Si}$	2.17	97.10	0.73	$6 \times 10^{17}$	$2 \times 10^{17}$
$^{30}\text{Si}$	0.67	0.59	98.74	$9 \times 10^{17}$	$5 \times 10^{17}$
$^{\text{nat}}\text{Si}$	92.2	4.7	3.1	$7 \times 10^{17}$	N.D. ( $<5 \times 10^{17}$ )

N.D., not detected.

6000–1000 spectra are co-added in order to improve the signal-to-noise ratio.

## 3. Experimental calculation

For the frequency calculation of the staggered (Si–O–Si–O–Si) and skewed (Si–O–Si–Si–O–Si) dimers based on the models suggested by Pesola et al. [15,16], a one-dimensional chain with five and 14 silicon atoms added to the both ends for staggered and skewed dimers, respectively was employed. For simplicity of calculation, 100% enrichments of  $^{28}\text{Si}$ ,  $^{29}\text{Si}$ , and  $^{30}\text{Si}$  are assumed for the  $^{\text{nat}}\text{Si}$ ,  $^{29}\text{Si}$ , and  $^{30}\text{Si}$  samples, respectively. Similarly, we assumed oxygen atoms are 100% of either  $^{16}\text{O}$  or  $^{18}\text{O}$ . The force constant  $k_1$  of Si–Si atom is 113.33 N/m as employed in the previous study of oxygen LVM in silicon [8]. The other force constants are determined based on the experimentally measured frequencies of dimers in  $^{\text{nat}}\text{Si}$ ,  $^{29}\text{Si}$ ,  $^{30}\text{Si}$ , and  $^{18}\text{O}$ -doped Si samples [13,15]. Some of the force constants have been determined assuming that the higher LVM frequency of the pair B overlaps with the peak position of isolated oxygen mode, as shown in Ref. [15].

## 4. Results and discussion

### 4.1. Experimental results

Figs. 2 and 3 show oxygen-related absorption peaks in the  $^{29}\text{Si}$ ,  $^{30}\text{Si}$ , and  $^{\text{nat}}\text{Si}$  samples, which show clear silicon-isotopic shifts (host-isotope effect) both at 5 K and room temperature. The sharp peaks in  $^{29}\text{Si}$  and  $^{30}\text{Si}$  around 1045  $\text{cm}^{-1}$  are the isolated oxygen peaks discussed by J. Kato et al. [7] and the peaks at 1044 and 1048  $\text{cm}^{-1}$  in  $^{\text{nat}}\text{Si}$  are thermal donor related [1].

Fig. 3 shows the spectra of  $^{29}\text{Si}$ ,  $^{30}\text{Si}$ , and  $^{\text{nat}}\text{Si}$  in the range of 1085–1110  $\text{cm}^{-1}$ . However, we should note that the C–O complex-related peaks also exist in these spectra. In  $^{\text{nat}}\text{Si}$ , the C–O complex peaks have been observed at 1104 and 1108  $\text{cm}^{-1}$  [19,20]. Therefore, it is possible that the host isotopic shift of C–O complex is similar to that of pair B. Indeed, observation of the peaks pair B (written as skewed dimer in Ref. [13]) was reported in carbon-rich silicon at 1105  $\text{cm}^{-1}$ , which is very close to the frequencies of the C–O complex [13]. The  $^{29}\text{Si}$  and  $^{30}\text{Si}$  samples also contain high carbon concentrations ( $10^{17}$  atoms/ $\text{cm}^3$ ).

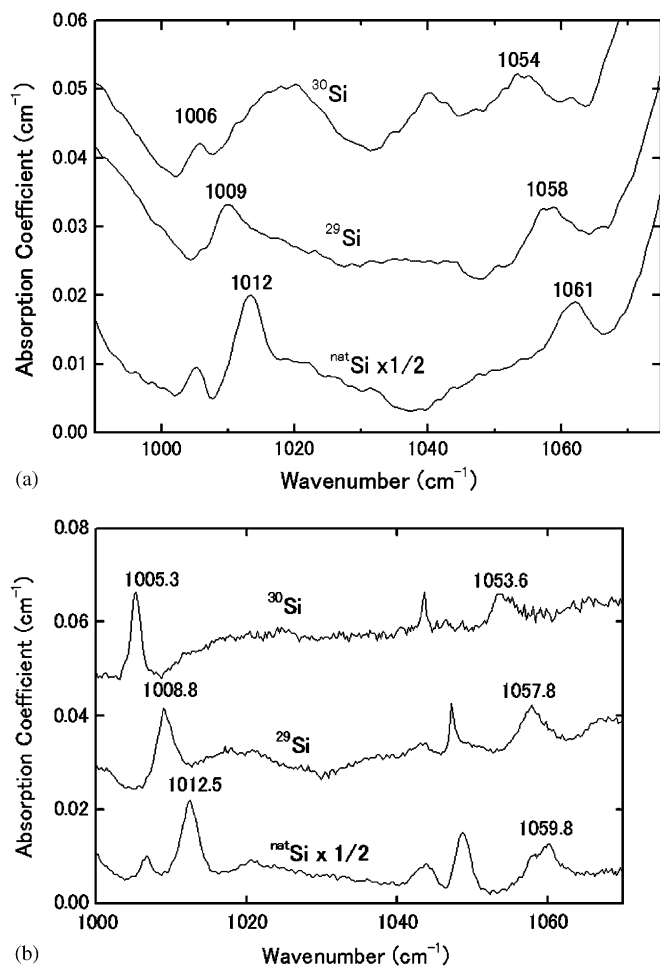


Fig. 2. Infrared absorption spectra of  $^{29}\text{Si}$ ,  $^{30}\text{Si}$ , and  $^{\text{nat}}\text{Si}$  samples in the range of  $990\text{--}1075\text{ cm}^{-1}$  recorded at (a) room temperature and (b) 5 K.

Furthermore, the intensity at  $1101$  and  $1098\text{ cm}^{-1}$  in  $^{29}\text{Si}$  and  $^{30}\text{Si}$ , respectively, are two times larger than the peak at around  $1105\text{ cm}^{-1}$ , whereas it is not so in  $^{\text{nat}}\text{Si}$  with the low carbon concentration. Therefore, some of the peaks in the  $^{29}\text{Si}$  and  $^{30}\text{Si}$  are composed of overlapping peaks of the pair B and C–O complexes. Similarly, the peaks at  $1101$  and  $1098\text{ cm}^{-1}$  may be composed of the pair B and C–O complex peaks. Nevertheless, let us compare the experimental peak positions with calculations for the pair B assuming that the peaks in Figs. 2 and 3 represent pair B peak positions.

#### 4.2. Calculation results

We performed calculation and assignment of the pairs A and B assuming two proposed configurations, staggered and skewed dimers, and compared with the experimentally obtained pairs A and B.

As a result, we achieved very good agreement between calculation assuming staggered dimers and experimental peak positions for both the absorption pairs A and B as shown in Table 2 with reasonable force constants shown in

Table 3. Therefore, both the pairs A and B may arise from the staggered dimers according to this simple analysis. Similar to the staggered dimers, we achieved very good agreement between the calculation assuming skewed dimers and experimental peak positions for the absorption pairs A and B as shown in Table 2 with reasonable force constants shown in Table 3. Thus, both the pairs A and B

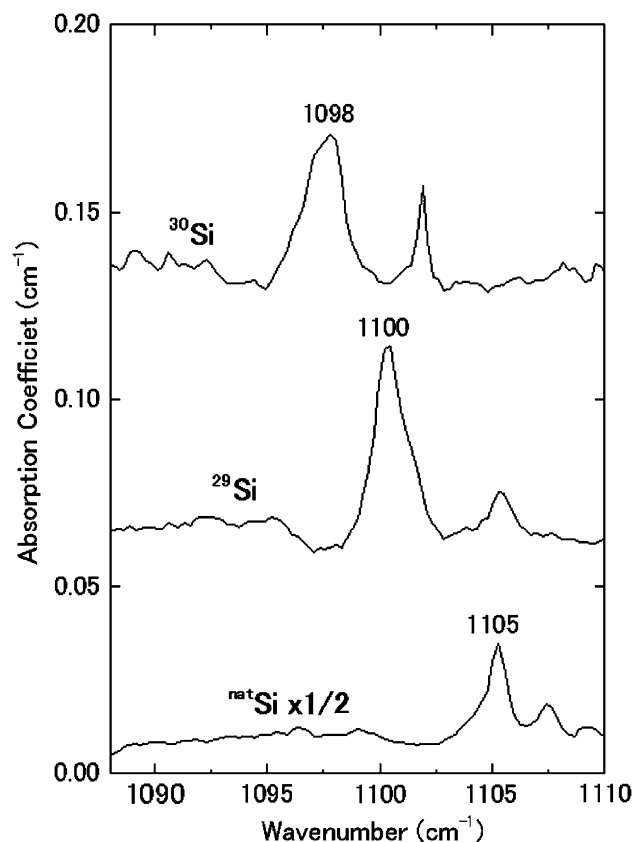


Fig. 3. Infrared absorption spectra of  $^{29}\text{Si}$ ,  $^{30}\text{Si}$ , and  $^{\text{nat}}\text{Si}$  samples in the range of  $1085\text{--}1110\text{ cm}^{-1}$  recorded at  $T = 5\text{ K}$ .

Table 2

Experimental results for the absorption pairs A and B and their comparison with calculated frequencies

	Experiment		Calculation			
	Pair A	Pair B	Staggered		Skewed	
			Pair A	Pair B	Pair A	Pair B
$^{\text{nat}}\text{Si}$	1059.8	1136.4	1060.4	1136.4	1060.2	1136.4
	1012.4	1105	1012.8	1105.6	1012.7	1105.3
$^{18}\text{O}$ -doped Si	1011.8	1084.4	1017.3	1087.3	1014.4	1090.6
	969.2	1057	971.7	1058.6	969.7	1060.7
$^{29}\text{Si}$	1057.8	1132.5	1055.3	1131.7	1055.9	1130.8
	1008.8	1101	1007.9	1100.8	1008.4	1099.8
$^{30}\text{Si}$	1053.6	1129.1	1050.5	1127.3	1051.8	1125.6
	1005.3	1098	1003.3	1096.4	1004.3	1094.6

Calculated frequencies include all of the combinations between staggered and skewed dimers and pairs A and B. Unit is wavenumber( $\text{cm}^{-1}$ ).

Table 3  
Force constants of each spring

		$k_2$	$k_3$	$k_4$	$k_5$	$k_6$
Staggered	Pair A	443.99	345.65	191.96	518.78	
	Pair B	521.13	388.05	171.36	651.86	
Skewed	Pair A	273.23	459.89	26.50	402.18	413.37
	Pair B	397.47	536.44	29.44	361.55	515.83

Unit is N/m.

may arise from the skewed dimers according to this simple analysis.

It has been shown that the simple one-dimensional harmonic model analysis is not capable of assignment of the pairs A and B as skewed or staggered dimers. Therefore, we shall have to rely on our physical intuition for the assignment of pairs A and B. It has been shown that the effect of the second nearest neighbor atoms on the LVM frequency shift is not so large for interstitial oxygen ( $\sim 1 \text{ cm}^{-1}$ ). This implies immediately that the frequency of the skewed dimers, which has silicon as the second nearest neighbor, is close to that of single oxygen LVM at  $1136 \text{ cm}^{-1}$ , i.e., the pair B is due to skewed dimers. The frequency of the staggered dimers, which share only one central silicon atom with two oxygen atoms, should be further away from  $1136 \text{ cm}^{-1}$  and therefore assigned to the pair A. Thus, previously suggested assignments of the staggered dimer for the pair A and the skewed dimer for the pair B is constituent with the present result [15].

## 5. Summary

We have investigated the host isotopic effect on LVM of oxygen dimers by FTIR in  $^{\text{nat}}\text{Si}$  and isotopically enriched  $^{29}\text{Si}$  and  $^{30}\text{Si}$  samples. The host isotopic shifts of LVM frequencies are clearly observed. We showed that one-dimensional harmonic potential calculation assuming the staggered and skewed dimers can both reproduce the experimentally observed LVM frequencies of pairs A and B. Therefore, we cannot assign whether A and B correspond to staggered and skewed simply from this comparison. However, further inspection shows that the pair A corresponds to staggered dimer LVM while the pair B corresponds to skewed dimer LVM.

## Acknowledgment

The authors wish to thank the Professor E.E. Haller for the fruitful discussion.

## References

- [1] C.S. Fuller, J.A. Ditzenberger, N.B. Hannay, E. Buehler, *Phys. Rev.* 96 (1954) 833.
- [2] P. Wagner, J. Hage, *Appl. Phys. A* 49 (1989) 123.
- [3] J.C. Mikkelsen Jr., S.J. Pearton, J.W. Corbett, S.J. Pennycook (Eds.), *Oxygen, Carbon, Hydrogen and Nitrogen in Crystalline Silicon*, Materials Research Society Symposia Proceedings, vol. 59, Materials Research Society, Pittsburgh, 1985.
- [4] F. Shimura (Ed.), *Oxygen in silicon, Semiconductors and Semimetals*, vol. 42, Academic Press, New York, 1994.
- [5] K. Takyu, K.M. Itoh, K. Oka, N. Saito, V.I. Ozhogin, *Jpn. J. Appl. Phys.* 38 (1999) L1493.
- [6] K.M. Itoh, J. Kato, M. Uemura, A.K. Kaliteyevskii, O.N. Godisov, G.G. Devyatych, A.D. Bulanov, A.V. Gusev, I.D. Kovalev, P.G. Sennikov, H.-J. Pohl, N.V. Abrosimov, H. Riemann, *Jpn. J. Appl. Phys.* 1 42 (2003) 6248.
- [7] J. Kato, K.M. Itoh, H. Yamada-Kaneta, H.-J. Pohl, *Phys. Rev. B* 68 (2003) 035205.
- [8] P.G. Sennikov, T.V. Kotereva, A.G. Kurganov, B.A. Andreev, H. Niemann, D. Schiel, V.V. Emtsev, H.-J. Pohl, *Semiconductors* 39 (2005) 300.
- [9] R.N. Pereira, T. Ohya, K.M. Itoh, B. Bech Nielsen, *Physica E* 340–342 (2003) 697.
- [10] J.L. Lindström, T. Hallberg, *Phys. Rev. Lett.* 72 (1994) 2729.
- [11] J.L. Lindström, T. Hallberg, *J. Appl. Phys.* 77 (1994) 2684.
- [12] T. Hallberg, J.L. Lindström, *J. Appl. Phys.* 79 (1996) 7570.
- [13] T. Hallberg, J.L. Lindström, L.I. Murin, V.P. Markevich, *Mater. Sci. Forum* 258–263 (1997) 361.
- [14] L.I. Murin, T. Hallberg, V.P. Markevich, J.L. Lindström, *Phys. Rev. Lett.* 80 (1998) 93.
- [15] M. Pesola, J. von Boehm, R.M. Nieminen, *Phys. Rev. Lett.* 82 (1999) 4022.
- [16] M. Pesola, J. von Boehm, T. Mattila, R.M. Nieminen, *Phys. Rev. B* 60 (1999) 11449.
- [17] Y.J. Lee, M. Pesola, J. von Boehm, R.M. Niemien, *Phys. Rev. B* 66 (2002) 075219.
- [18] A. Baghdadi, W.M. Bullis, M.C. Croarkin, Y.-Z. Li, R.I. Scace, R.W. Series, P. Stallhofer, M. Watanabe, *J. Electrochem. Soc.* 136 (1989) 2015.
- [19] Y. Shirakawa, H. Yamada-Kaneta, H. Mori, *J. Appl. Phys.* 77 (1995) 41.
- [20] Y. Shirakawa, H. Yamada-Kaneta, *J. Appl. Phys.* 80 (1996) 4199.